Biosystems Engineering 255 (2025) 104159

Contents lists available at ScienceDirect

Biosystems Engineering

journal homepage: www.elsevier.com/locate/issn/15375110

Research Paper

Unveiling host-seeking behaviour in entomopathogenic nematodes via lab-on-a-chip technology

Gianluca Manduca [a,b,*], Valeria Zeni [c], Anita Casadei [a,b], Eustachio Tarasco [d], Andrea Lucchi [c], Giovanni Benelli [c], Cesare Stefanini [a,b], Donato Romano [a,b,**]

[a] The BioRobotics Institute, Sant'Anna School of Advanced Studies, Viale R. Piaggio 34, Pontedera, 56025, Pisa, Italy
[b] Department of Excellence in Robotics and AI, Sant'Anna School of Advanced Studies, Piazza Martiri della Libertà 33, 56127, Pisa, Italy
[c] Department of Agriculture, Food and Environment, University of Pisa, Via del Borghetto 80, 856124, Pisa, Italy
[d] Department of Soil, Plant and Food Sciences, University of Bari Aldo Moro, Via Amendola 165/A, 70126, Bari, Italy

ARTICLE INFO

Keywords:
Biological control
Deep learning
European grapevine moth
Integrated pest management
Lab-on-a-chip
Steinernema carpocapsae

ABSTRACT

Entomopathogenic nematodes (EPNs) can be employed as biological control agents (BCAs) for many insect pests' sustainable management. Despite their widespread use, our understanding of EPNs biology, particularly interactions with their hosts, remains limited. Advancing knowledge of EPNs ecology and host interactions is crucial for optimising their efficacy in pest management. This study pioneers an interdisciplinary approach, at the interface of engineering and applied entomology, to investigate the behaviour of the EPN *Steinernema carpocapsae*. A novel method combining microfluidics, machine learning, and optical flow is presented. A lab-on-a-chip platform was designed to enable accurate investigation of EPN response to stimuli. A convolutional neural network (CNN) identified nematodes and distinguished their responses to host-derived cues achieving 0.94 accuracy and 1.00 precision in detecting stimulus presence at video-level, classifying EPN behaviour within a controlled environment that simulates host conditions. Optical flow analysis revealed differences in motor activity of EPN upon exposure to stimuli, providing new insights into their dynamic responses. *Steinernema carpocapsae* exhibited more intense activity in presence of host-borne cues ($p = 0.0055$). Support vector machine (SVM) and multilayer perceptron (MLP) classifiers distinguished stimulus contexts from optical flow features, with an area under the receiver operating characteristic (ROC) curve of 0.71. These results highlight that, although *S. carpocapsae* is typically considered an ambusher, it may actively engage in host-seeking behaviour, suggesting a shift in our understanding of its search strategies. This methodology significantly enhances the detection and understanding of EPN responses to cues, advancing their potential in precision biocontrol programs for sustainable pest management actions.

Science4Impact statement (S4IS): This study develops a novel lab-on-a-chip platform integrating artificial intelligence (AI) for the precise investigation of host-seeking behaviours in the entomopathogenic nematode *Steinernema carpocapsae*, a biological control agent (BCA) with potential for sustainable pest management. By combining microfluidic design with deep learning, the platform accurately assesses nematode responses to host-derived cues, providing new insights into its foraging adaptability beyond conventional techniques. This research can help researchers and agricultural stakeholders by enhancing understanding of BCA behaviour, optimising pest control applications, and informing evidence-based decisions on sustainable crop protection. The findings also support quality assurance in biological control validation by offering a rigorous framework for evaluating nematode effectiveness under realistic conditions, promoting its broader adoption in integrated pest management strategies.

* Corresponding author. The BioRobotics Institute, Sant'Anna School of Advanced Studies, Viale R. Piaggio 34, Pontedera, 56025, Pisa, Italy.
** Corresponding author. The BioRobotics Institute, Sant'Anna School of Advanced Studies, Viale R. Piaggio 34, Pontedera, 56025, Pisa, Italy.
E-mail addresses: gianluca.manduca@santannapisa.it (G. Manduca), donato.romano@santannapisa.it (D. Romano).

https://doi.org/10.1016/j.biosystemseng.2025.104159
Received 24 April 2024; Received in revised form 10 April 2025; Accepted 12 April 2025
Available online 9 May 2025

Nomenclature

Abbreviations	
AI	Artificial intelligence
AUC	Area under the curve
BCA	Biological control agent
CAD	Computer-aided design
CLAHE	Contrast limited adaptive histogram equalisation
CNN	Convolutional neural network
CV	Cross-validation
EGVM	European grapevine moth
EPN	Entomopathogenic nematode
GFLOPS	Giga floating-point operations per second
GPU	Graphics processing unit
IoU	Intersection over union
mAP	Mean average precision
MB	Megabytes
MLP	Multilayer perceptron
MP	Megapixels
PDMS	Polydimethylsiloxane
RBF	Radial basis function
RGB	Red-green-blue
ROC	Receiver operating characteristic
SVM	Support vector machine
UAV	Unmanned aerial vehicle
Symbols	
A_1, A_2	Quadratic polynomial coefficient matrices
b_1, b_2	Polynomial coefficient vectors
c_1, c_2	Polynomial constant terms
d	Displacement vector [px] (pixels)
d_t	Time step [s] (seconds)
d_x	Distance step along the x-axis [px]
d_y	Distance step along the y-axis [px]
f_x	Image gradient along the x-axis
f_y	Image gradient along the y-axis
f_t	Image gradient along the time
$I(x,y,t)$	Pixel intensity at coordinates (x,y) and time t
N	Total number of classes
u	Optical flow component along the x-axis [px/s]
v	Optical flow component along the y-axis [px/s]
X	Vector of coordinates $(x,y)^T$
FN	False negatives number
FP	False positives number
FPR	False positive rate
TN	True negatives number
TP	True positives number
TPR	True positive rate

1. Introduction

The entomopathogenic nematode (EPN) *Steinernema carpocapsae* Weiser (Rhabditida: Steinernematidae), has gained a growing attention for its potential as an effective biological control agent (BCA) against a number of arthropod pests (Lalitha et al., 2022; Tarasco et al., 2023). Traditionally reported as an 'ambusher' species, *S. carpocapsae* is thought to target highly mobile, surface-dwelling pests due to its habit of accumulating near the soil surface (Campbell & Gaugler, 1997). However, several studies challenge this hypothesis, suggesting that *S. carpocapsae* can be effective in controlling a broader range of pests, including those living deep within the substrate or exhibiting cryptic behaviour (Gang & Hallem, 2016; Wilson et al., 2012). Despite its potential as a BCA, the widespread acceptance of *S. carpocapsae* ambush-foraging strategy has led to its dismissal in certain pest control scenarios (Gaugler, 1988; Koppenhöfer & Kaya, 1996). Consequently, it is crucial to reassess and expand our understanding of the foraging behaviour of this EPN, particularly in contexts diverging from conventional soil environments (Stuart et al., 2015).

Microfluidics and lab-on-a-chip technologies represent a paradigm shift in scientific instrumentation, offering unparalleled versatility and efficiency (Romano et al., 2022; Shanti et al., 2018). This transformative approach is revolutionising many research contexts, including genomic analysis, diagnostics, and environmental monitoring, promoting groundbreaking discoveries (Campana & Wlodkowic, 2018; Conde et al., 2016). Through precise fluidic control and reduced sample/reagent volumes, lab-on-a-chip platforms enhance experimental throughput and minimise waste (Sengupta & Hussain, 2022). In addition, rapid prototyping methods like 3D printing, micromachining, laser cutting, expedite device fabrication fostering innovation agility (Garmasukis et al., 2023).

Recent advancements in artificial intelligence (AI) and automation are driving substantial technological progress, influencing social, healthcare, industrial, and environmental sectors (Ferreira et al., 2023). These approaches provide robust solutions to complex challenges and can offer tailored strategies for dynamic challenges in pest management and crop protection science (Manduca et al., 2023a; Mesías-Ruiz et al., 2023). Among these, deep learning techniques have demonstrated notable capabilities in a wide range of applications, from detecting and classifying insect species (Santaera et al., 2025) to recognising animal actions (Fazzari, Romano, Falchi, & Stefanini, 2025).

This study introduces a novel lab-on-a-chip platform integrated with AI to investigate the behavioural patterns of *S. carpocapsae* in response to host-borne cues, overcoming the limitations of traditional observational methods. A convolutional neural network (CNN) model was employed to identify nematodes and analyse their behaviour in response to host-borne stimuli. Optical flow analysis was integrated to assess motor activity, offering deeper insights into host detection and exploitation mechanisms. Additionally, machine learning classifiers were employed to categorise nematode motor activity based on features extracted from optical flow data. Fig. 1 presents a workflow of the proposed approach. It is hypothesised that *S. carpocapsae* exhibits a more flexible and adaptable host-seeking behaviour than traditionally assumed, responding to a broader range of host-derived stimuli. A deeper understanding of the nematode's foraging strategies could enhance its effectiveness as a BCA against key insect pests, contributing to sustainable crop protection.

2. Materials and methods

2.1. Steinernema carpocapsae

EPNs at the infective juvenile stage (IJ) were tested, using NEMOPAK SC, a commercial product kindly supplied by Bioplanet (Cesena, Italy). The nematode's body measures approximately 400–500 μm in length and 30 μm in width, as reported by Shinde et al. (2010). The EPNs were stored at 4–8 °C to maintain their viability and were reconstituted in distilled water prior to experimentation. EPNs were placed in water at 25 °C to activate them, where they were subjected to continuous agitation using a magnetic vortex for 20 min. This procedure was selected to reproduce environmental conditions promoting the nematode activity, thus ensuring optimal responsiveness.

2.2. Tested cues

Herein, host-borne cues derived from moth larval faeces were chosen, as these cues are known to play a significant role in the host-seeking behaviour of several EPNs (Baiocchi et al., 2017). The reasoning behind this choice lies in the natural interactions between EPNs and their preferred hosts, as the chemical signals present in the faeces can potentially elicit behavioural responses from this nematode species. Earlier research reported the attractiveness shown by various cues on EPN behaviour (Jagodič et al., 2017; Zhang et al., 2021). In particular, the attraction triggered by host-borne cues, such as the host gut content, has been noted (Grewal et al., 1993).

As host-borne cues, faeces of 5th instar larvae of the European grapevine moth (EGVM), *Lobesia botrana* (Den. & Schiff.) (Lepidoptera: Tortricidae), a primary pest of grapevine (Benelli et al., 2023a, 2023b), were used. EGVM larvae were reared in the laboratory on an artificial diet as detailed by Benelli et al. (2020).

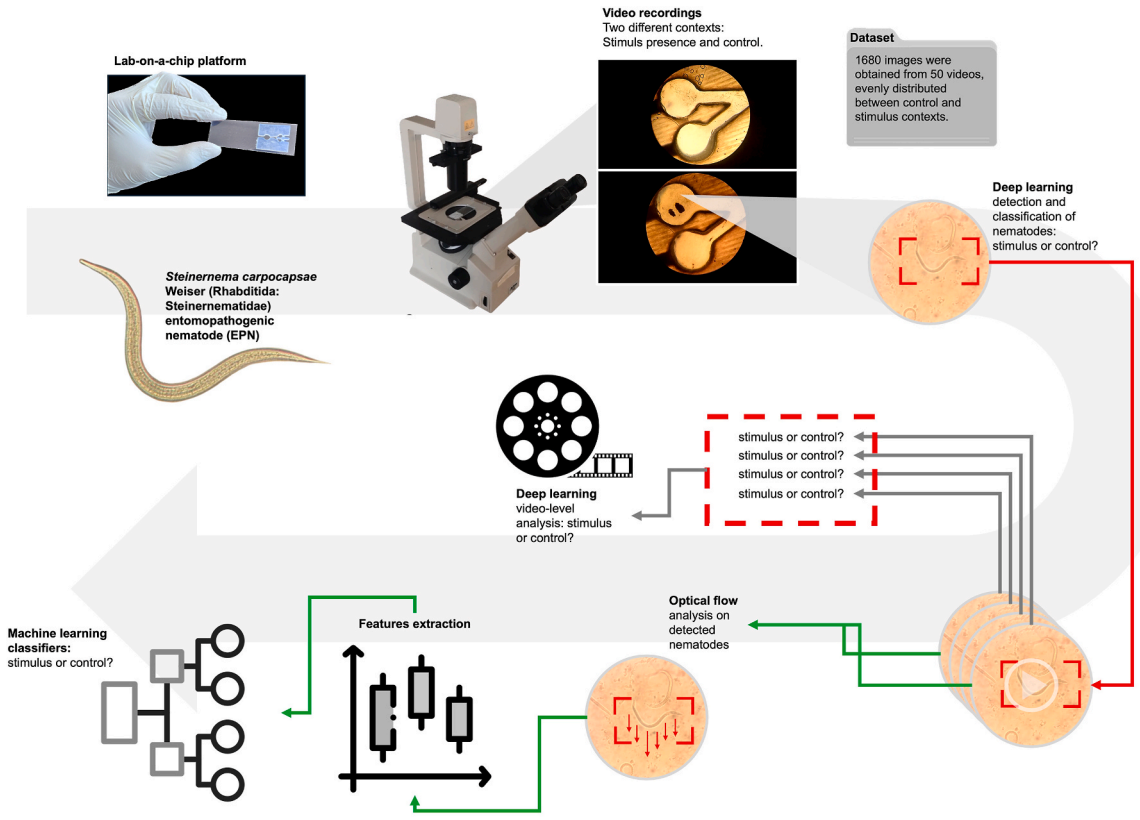

Fig. 1. Workflow of the proposed approach: Design of the lab-on-a-chip device and visual representation of the entomopathogenic nematode *Steinernema carpocapsae*. The experimental setup is then presented, where the nematodes are exposed to stimuli. Data are subsequently collected and analysed using learning algorithms and optical flow to assess the nematodes' responses to host stimuli.

2.3. Lab-on-a-chip design

The lab-on-a-chip device was designed and fabricated to provide a controlled environment suitable to the analysis of EPN behaviour. Fig. 2 presents the design and fabrication of the platform. The design of the miniaturised two-choice arena was produced by using the computer-aided design (CAD) software SolidWorks (Dassault Systemes, Velizy Villacoublay, France), ensuring precise dimensions and functionality. Subsequently, the fabrication of the microfluidic arena was obtained through rapid prototyping techniques, employing a biocompatible resin (VisiJet® M3 Crystal, 3D Systems). This setup is essential for investigating the parasitic behaviour and locomotion of EPNs in an environment that mimics their natural habitat and enhances their visibility (Wolozin et al., 2011).

The microfluidic arena was crafted to feature a releasing chamber (diameter = 5 mm; height = 2 mm) and two chambers that can potentially contain selected cues (diameter = 3 mm; height = 2 mm). The design of the arena allows for the exploration of EPN's behaviour without imposing spatial constraints on their motility, thereby minimising potential biases. Each chamber is seamlessly connected to the releasing chamber through dedicated aisles (length = 3 mm for the horizontal branch; length = 4 mm for the oblique branch; width = 1 mm; height = 2 mm), forming a Y-maze arena configuration. To facilitate observation and recording of *S. carpocapsae* behaviour, the floor of the lab-on-a-chip consists of a transparent glass plate firmly glued to the base of the upper component. This connection was obtained by depositing a polydimethylsiloxane (PDMS) film (Sylgard 184) with a curing time of 1 h at 100 °C (Johnston et al., 2014), ensuring stability and optical transparency throughout the experimentation process. The dimensions and the architectural design of the platform were selected to achieve optimal positioning beneath the inverted microscope (Nikon TMS Inverted, Nikon, Japan). Overall, the novel lab-on-a-chip is 75 mm in length and 25 mm in width.

2.4. Experimental procedure and recordings

During experimentation, around 10 *S. carpocapsae* individuals were introduced into the releasing chamber using a pipette, enabling precise control over their placement within the microfluidic system. The number of nematodes selected was compatible with the dimensions of the platform's channels, facilitating detailed morphological and behavioural analysis of the species. The microfluidic platform was positioned under a high-resolution 3D visual inspection microscope equipped with a total magnification of 25×. The overall setup facilitated detailed observation of EPN behaviour within the microfluidic system, enabling accurate recording of their responses to host-related cues provided within the chambers. The utilisation of this microfluidic platform ensured the recording of reliable and reproducible data, crucial for investigating the mechanisms underlying EPN behaviour and responses to selected stimuli. Prior to testing, several preparatory steps were undertaken. The chip was washed with water and 70 % ethanol to remove contaminants, reduce surface tension, enhance arena wettability, and improve nematode locomotion. A second washing was carried out using water to eliminate the alcohol traces potentially harmful to the EPN. The chip was then filled with the medium, i.e., 0.9 % NaCl physiological solution, since it is useful to avoid osmotic stress. For the cue attraction tests, faeces from 5th instar EGVM larvae were collected from rearing boxes using a Pasteur pipette and transferred to a separate container that had been previously cleaned with ethanol and left to air dry accurately. The host-borne cue (i.e. 0.07 ± 0.008 mg of EGVM faeces) was positioned in the opposite arenas, alternating localisation, and flipping the arena to avoid any positional bias during the trials. Videos were recorded under the microscope for a total of 5 min. Video analysis considered only 60 s recording to avoid acclimation time and promote next

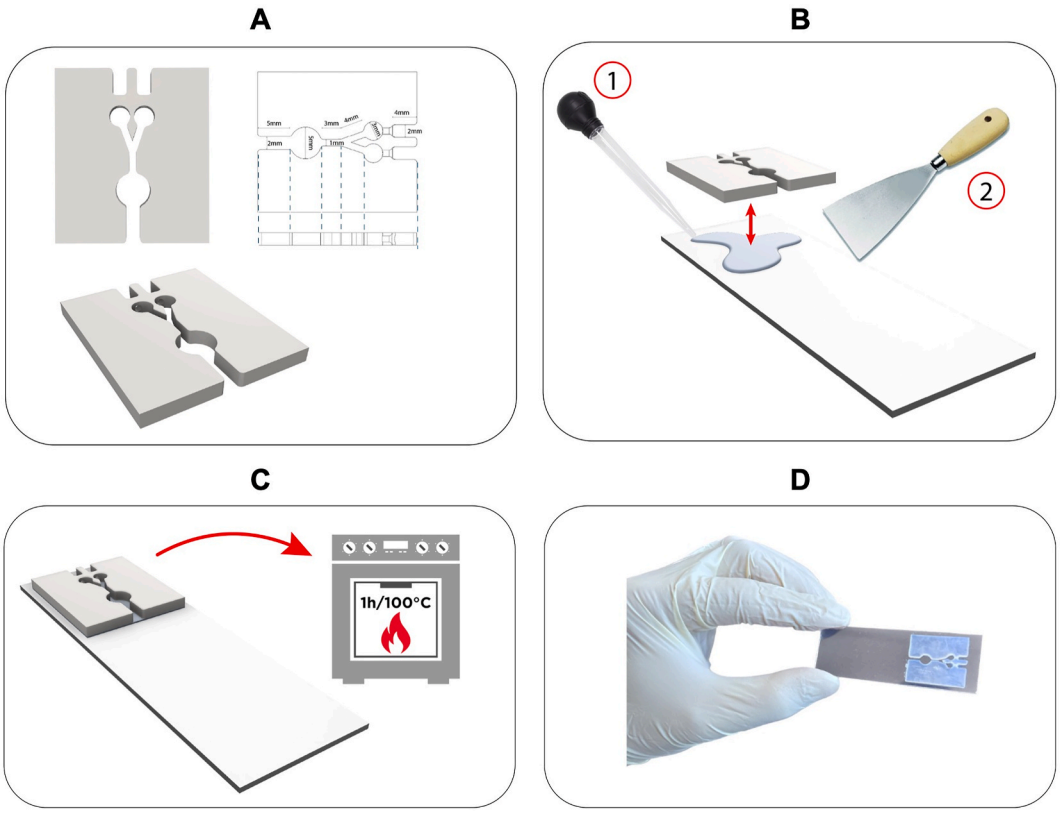

Fig. 2. Lab-on-a-chip platform design and fabrication: Design and dimensions of the chip (**A**); assembly of the chip components involves spreading a thin layer of Sylgard 184 onto the glass slide, followed by placing the biocompatible resin chip on top of the PDMS layer, ensuring proper alignment and adhesion (**B**); the platform is cured in the oven at 100 °C for 1 h to increase Sylgard transparency and resistance (**C**); fabricated microfluidic platform ready to be employed (**D**).

computer vision and deep learning analysis. Videos were recorded by using a red-green-blue (RGB) camera (48 MP, aperture f-number 1.8) set on the microscope. Following each test, the device was washed and cleaned following the above-described procedures.

2.5. Deep learning detection

A deep learning approach was used to distinguish a context in the presence of a host-borne stimulus based on the behaviour of EPNs. This approach enabled clear differentiation between these contexts and facilitated the analysis of motion variations captured in images, which were attributed to the presence of the stimulus. Nematodes served as biosensors, gathering information about their surrounding environment, while concurrently enabling the investigation of changes in behavioural traits in response to stimuli with the proposed deep learning approach.

A YOLOv8n CNN model, pre-trained on the COCO dataset, a widely recognised benchmark for object detection tasks (Terven et al., 2023), was used. The choice of this CNN model was based on its versatility and proven effectiveness in object detection. YOLO networks, especially the v8 version, have been successfully deployed across a wide spectrum of detection challenges. These include tasks like identifying small objects in unmanned aerial vehicle (UAV) images (Huangfu and Li, 2023), assessing compliance with medical face mask usage in COVID-19 contexts (Ferreira, do Couto, & de Melo Baptista Domingues, 2024), and detecting various marine species (Manduca et al., 2023b). These examples highlight the adaptability and effectiveness of the YOLOv8 model across different applications. YOLOv8 employs a CNN architecture structured into three primary components: the backbone, neck, and head. The backbone, which is based on a modified CSPDarknet53 architecture, is responsible for extracting features from the input image. The neck merges feature maps from different stages of the backbone to capture information at various scales. The head predicts bounding boxes, objectness scores, and class probabilities for each grid cell in the feature map using multiple detection modules, which are then aggregated to produce the final detections. A key characteristic of YOLOv8 is its operation as an anchor-free detection model. In its v8n version, the model weighs 6.24 MB. The pre-trained CNN model was fine-tuned to specifically identify and differentiate nematodes exposed to a stimulus from those in a control setting. A dataset comprising 1680 images was curated from 50 videos, evenly distributed between control and stimulus contexts. The dataset was partitioned into training (1189 images), validation (339 images), and test (152 images) sets. Images were manually labelled using the Makesense software. The dataset also included approximately 10 % background images without EPN, proportionally allocated across the three sets. The CNN training process used a batch size of 8 for 200 epochs. Data augmentation was considered. The Mosaic method was used to create a diverse input by combining four resized images into a single mosaic. Both uniform and median blurring were applied with a randomly chosen kernel size between 3 and 7 and a 0.01 probability of use. Additionally, grayscale conversion was applied with a 0.01 probability, along with contrast limited adaptive histogram equalisation (CLAHE) for further augmentation, using a clip limit of 4 and a tile grid size of 8x8.

Using the fine-tuned CNN model, a comprehensive analysis was conducted on 32 inference videos, each lasting 1 min and evenly divided between stimulus and control contexts. Frames were systematically extracted at a rate of 1 Hz, and for each frame, the CNN was applied to detect EPN under both conditions. The CNN detects and differentiates the nematodes in the arena into two classes based on their behaviour: control and stimulus. The results were aggregated to assess the presence or absence of a stimulus in each scenario, allowing for a comprehensive differentiation throughout the entire video. A prediction value of 0 corresponds to the control condition, while a value of 1 indicates the presence of a stimulus. For each frame, the average of the predictions

was calculated. Subsequently, the average across all frames was computed to provide a single value representing each video. This iterative process was repeated for all videos, ensuring thorough analysis. The CNN training and subsequent analyses were performed using Ultralytics in Python, leveraging a Tesla T4 graphics processing unit (GPU).

2.6. Optical flow analysis

Motor analysis was conducted employing an optical flow approach and the Farnebäck algorithm (Farnebäck, 2003). This methodology, widely recognised for its effectiveness, has been applied across different domains. For instance, in fire detection (Fatichah et al., 2019), or for recognition and localisation of anomalous events in crowd scenes contributing to enhanced security measures and crowd management strategies (Alhothali et al., 2023). Moreover, the application of optical flow analysis extends to driving scenarios, where it plays a crucial role in various applications (Ping et al., 2023). Additionally, its utility in violence detection (Mumtaz et al., 2023) underscores its significance in public safety and security initiatives.

Optical flow represents the apparent motion of objects between two frames. Optical flow methods operate by analysing variations in intensity across both space and time $I(x,y,t)$. When an object moves, its pixel intensity shifts by a displacement (dx,dy) over a time step dt. Assuming that the intensity of the object remains constant between frames, it results:

$$I(x,y,t) = I(x+dx, y+dy, t+dt). \tag{1}$$

By applying a first-order Taylor series expansion, it results:

$$I(x+dx,y+dy,t+dt) = I(x,y,t) + \frac{\partial I}{\partial x}dx + \frac{\partial I}{\partial y}dy + \frac{\partial I}{\partial t}dt. \tag{2}$$

From Eqs. (1) and (2) it is possible to obtain the constraint equation:

$$\frac{\partial I}{\partial x}\frac{dx}{dt} + \frac{\partial I}{\partial y}\frac{dy}{dt} + \frac{\partial I}{\partial t} = 0. \tag{3}$$

$f_x = \frac{\partial I}{\partial x}$, $f_y = \frac{\partial I}{\partial y}$, and $f_t = \frac{\partial I}{\partial t}$ are the image gradients along the x-axis, y-axis, and time. $u = \frac{dx}{dt}$ and $v = \frac{dy}{dt}$ are the unknown variables.

The Farnebäck method uses polynomial expansion so that some neighbourhood of each pixel is approximated by using a quadratic polynomial:

$$I_1(X) = X^T A_1 X + b_1{}^T X + c_1, \tag{4}$$

where $X = (x,y)^T$. A new signal is constructed over a displacement d:

$$\begin{aligned} I_2(X) &= I_1(X-d) = (X-d)^T A_1 (X-d) + b_1{}^T (X-d) + c_1 \\ &= X^T A_1 X + (b_1 - 2A_1 d)^T X + d^T A_1 d - b_1{}^T d + c_1 \\ &= X^T A_2 X + b_2{}^T X + c_2, \end{aligned} \tag{5}$$

where,

$$A_2 = A_1, \tag{6}$$

$$b_2 = b_1 - 2A_1 d, \tag{7}$$

$$c_2 = d^T A_1 d - b_1{}^T d + c_1. \tag{8}$$

From Eq. (7), in case of non-singular A_1, the displacement can be computed:

$$d = -\frac{1}{2} A_1{}^{-1} (b_2 - b_1). \tag{9}$$

In this study optical flow analysis was coupled with deep learning detection to access the motor activity of nematodes during experiments. Fig. 3 presents a graphical representation of the entire process. Deep learning was used to identify nematodes in the arena by defining bounding boxes around them, while optical flow analysis was applied to focus on these detected areas and quantify their movement intensity. This analysis aimed to compare the nematodes' movement in response to different conditions: with and without cues. The procedure is detailed below. First, video frames were converted from RGB to grayscale. Optical flow between consecutive frames was computed, focusing on both the magnitude and direction of motion; however, only the magnitude was used for this analysis. Optical flow calculations were conducted with the Python OpenCV library and the calcOpticalFlowFarneback(.) function. The parameters were set as follows: scale = 0.5, number of pyramid layers = 5, averaging window size = 15, number of iterations = 3, pixel neighbourhood size used for polynomial expansion at each pixel = 7, and standard deviation of the Gaussian used to smooth derivatives for polynomial expansion = 1.5.

A total of 60 videos were considered, balanced between control and stimulus conditions. Given that nematodes exhibit body movements with a 2 Hz frequency according to literature (Buckingham et al., 2014), frames were sampled at 5 Hz for the optical flow analysis, in accordance with the Shannon theorem. The optical flow magnitude was computed by comparing two frames. The CNN model was used to obtain bounding boxes around each detected nematode. The average magnitude of motion was computed within each bounding box. Then, among the average magnitude values computed within each bounding box, the maximum and average values for each frame were considered. The maximum value was chosen to emphasise the most pronounced nematode movements, reducing the risk of considering background areas misclassified as EPNs

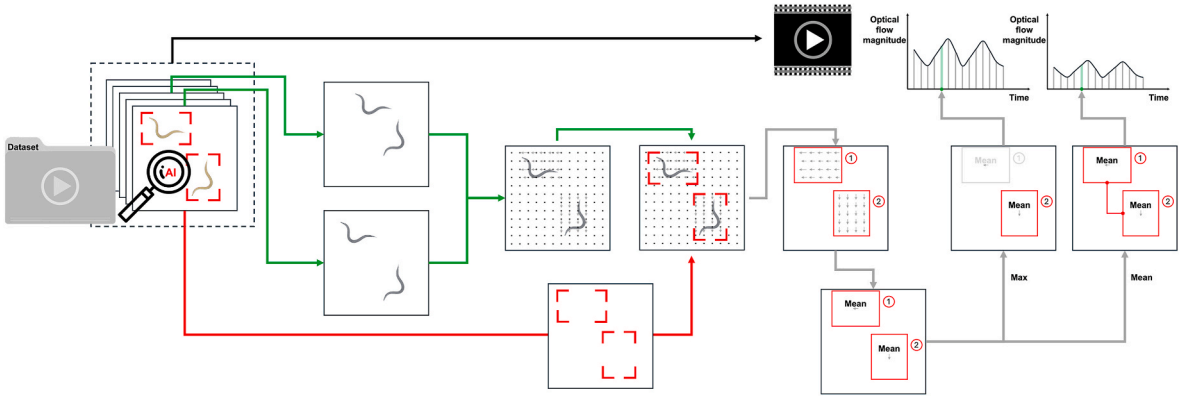

Fig. 3. Optical flow analysis: Schematic representation of the entire process used to analyse nematodes' motor activity through optical flow. Starting from a video dataset, optical flow is computed from frames comparison, focusing on detected nematodes. Two strategies are employed to extract optical flow magnitude profiles for each video to investigate nematodes' movement dynamics.

during the analysis, while the average value offered a more comprehensive view of movement throughout the entire experiment. Temporal data were collected, and three features—mean, maximum, and variance—were extracted to provide a comprehensive measure of motion for each video, considering both strategies used for temporal data extraction.

2.7. Statistical analysis

Data were normally distributed (Shapiro-Wilk test, $p > 0.01$) and homoscedastic (Levene test, $p > 0.01$). Statistical significance between stimuli and control was established using a *t*-test. Statistical analyses were performed using JMP Pro 17 software. The threshold was set at $p = 0.05$.

2.8. Machine learning classifiers

Following the statistical analysis, significant features were selected to train various machine learning models aimed at distinguishing EPN motor activity in response to stimuli, based on features extracted from optical flow data. Two models were considered: Support vector machine (SVM) and multilayer perceptron (MLP). To ensure robust testing, nested cross-validation (CV) was employed, incorporating both 4-fold external and internal loops. Hyperparameter tuning was carried out using grid search CV. All analyses were conducted using scikit-learn in Python. For SVM, both radial basis function (RBF) and linear kernels were considered, along with a range of C values from 0.01 to 10. For MLP, a maximum of four nodes with a single hidden layer were tested.

2.9. Performance assessment

When evaluating the performance of the AI models, multiple metrics were considered. Accuracy quantifies the ratio of correct predictions made by the model against the total number of predictions.

Precision denotes the likelihood of accurately predicting positive samples among those predicted as positive. It is computed using the following formula:

$$Precision = \frac{TP}{TP + FP}. \tag{10}$$

The variable TP represents the number of true positives, while FP represents the number of false positives.

Recall denotes the probability of accurately predicting positive samples among all actual positive samples. It is calculated as follows:

$$Recall = \frac{TP}{TP + FN}. \tag{11}$$

The variable FN denotes the count of false negatives.

The F1-score provides the harmonic mean of precision and recall, thus offering a balanced evaluation that considers both metrics. It can be computed as follows:

$$F1 - Score = 2 \cdot \frac{Precision \cdot Recall}{Precision + Recall}. \tag{12}$$

The mean average precision (mAP) is a performance metric used in object detection tasks. It is calculated using the following formula:

$$mAP = \frac{\sum_{n=1}^{N} AP_n}{N}. \tag{13}$$

N represents the total number of classes, and AP_n denotes the average precision of class n, which corresponds to the area under the precision-recall curve. mAP@0.5 denotes the mean average precision at an intersection over union (IoU) threshold of 0.5. IoU is a metric used to quantify the overlap between a predicted bounding box and the ground truth bounding box, calculated as the ratio of the intersection area to the union area of the two boxes. The receiver operating characteristic (ROC) curve plots the true positive rate (sensitivity) against the false positive rate (1-specificity) at various threshold values. The area under the curve (AUC) offers a comprehensive evaluation of the classifier's performance across all thresholds.

3. Results

Microscopic observations enabled the identification of key behaviours exhibited by EPNs, including increased movement and larger oscillation size. These investigations were made by using 25× total magnification and considering a circular area of 7 mm of diameter to be able to focus on the final part of the device. These observations indicate that the presence of host-borne cues influences the behavioural complex of *S. carpocapsae*. When placed in presence of the EGVM faeces, EPNs tended to increase their speed and turning rate, sometimes also crossing the entire central channel of the platform to reach the opposite chamber where the attractive cue was previously positioned. Indeed, control nematodes were less motile, moving with less broad oscillations; they rarely tried to cross the microfluidic platform. All these features had to be analysed by means of innovative and automated techniques to have a clear description of EPN's responses to a new potentially attractive cue. The EPNs directional change towards *L. botrana* faeces highlights the attractiveness of the selected cue. This aspect, though not well known in existing literature, is crucial for deepening our understanding of the species' behaviour and for optimising its use as a biological control agent.

The convolutional neural network has been trained to identify nematodes within the arena, but its capabilities extend further. Indeed, the network has been trained to distinguish stimulated EPNs. Training took 5.04 h over 200 epochs on a Tesla T4 GPU. The final model consists of 168 layers with 3,006,038 parameters, with a computational requirement of 8.1 giga floating-point operations per second (GFLOPS). Overall, the model achieved a precision of 0.63, recall of 0.62, and a mAP at 0.50 threshold of 0.61 on the validation set. For the control class, 0.79 of the samples were correctly classified, with 0.07 misclassified as stimulus and 0.14 as background. For the stimulus class, 0.70 of the samples were correctly classified, while 0.06 were misclassified as control and 0.24 as background. Fig. 4 presents 12 sample images from the test set, showing the network's detections. The images are evenly divided between stimulation and control conditions. As illustrated, the model identified nematodes within the arena and classified them based on their behaviour, distinguishing between stimulated and control.

Results suggest that the presence of the stimulus may induce changes in movement, thereby validating the behavioural variations observed. The results improve when aggregating frame-level data to a broader video-level analysis. Fig. 5**A** presents the predictions from the video analysis. A model prediction value of 0 corresponds to the control condition, while a value of 1 indicates the presence of a stimulus. For each frame, the average of the predictions was calculated. Subsequently, the average across all frames was computed to provide a single value representing each video. As shown in the normalised confusion matrix in Fig. 5**B**, the model distinguishes EPN's behaviours across various contexts within the video data. All control videos were correctly classified. Meanwhile, 0.88 of the videos with stimulus presence were correctly classified, with 0.12 misclassified as control. Fig. 5**C** presents the overall results across the different evaluation metrics. The model achieved an accuracy of 0.94, with a precision of 1.00, a recall of 0.88, and an F1-score of 0.93.

Subsequent optical flow analysis aims to delve deeper into dynamic variations in motor activity among EPNs in stimulus presence. Bounding boxes were generated for each video frame using the CNN model, and optical flow magnitude was calculated between consecutive frames. Fig. 6**A** illustrates two consecutive frames from a sample video with stimulus presence, showing detected EPNs and visualising the optical flow magnitude between them using MIN-MAX normalisation to

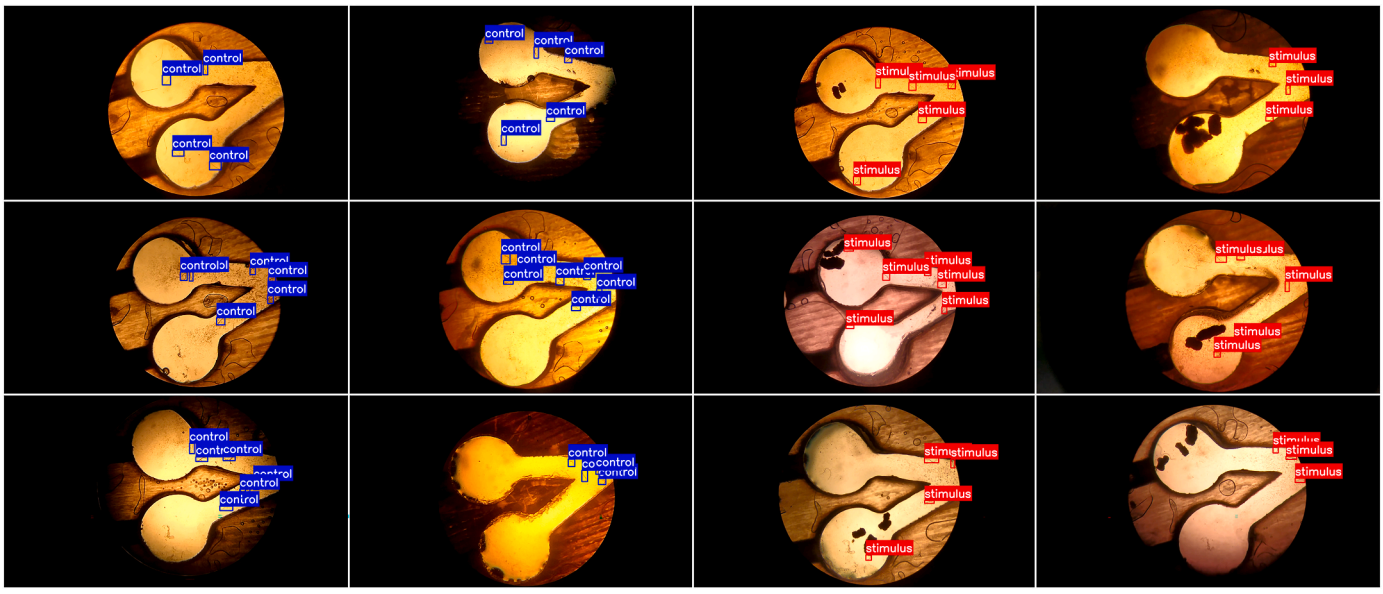

Fig. 4. Detections on the test set: 12 sample images showing the model's detections, evenly distributed between the stimulus and control conditions. The images are divided into two sets: 6 images from a control context (first and second columns, from left to right) and 6 images from a stimulus context (third and fourth columns). These examples demonstrate the model's ability to identify nematodes and classify their behaviour in response to the presence or absence of a stimulus.

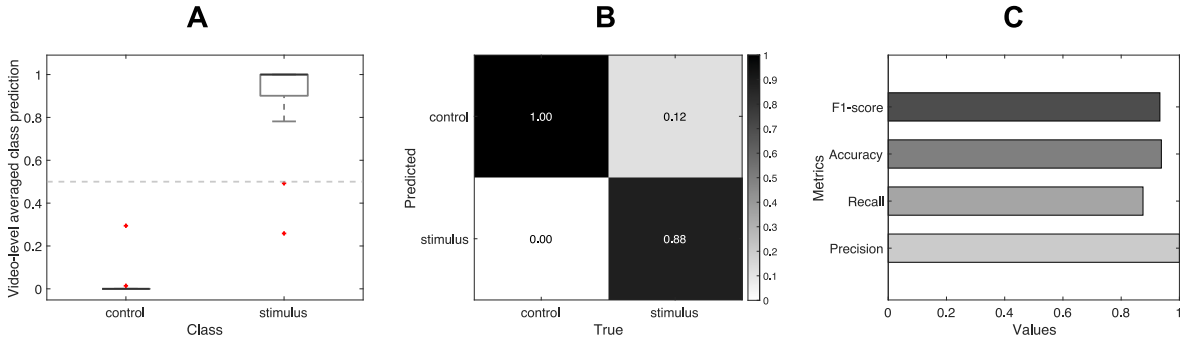

Fig. 5. Video-level results: Averaged class prediction values (**A**); normalised confusion matrix (**B**); overall results across the different evaluation metrics (**C**).

highlight motor activity. The average values within each bounding box were recorded, and the maximum and mean values were computed for each frame to construct temporal profiles across the video. These temporal profiles for the same sample video are shown in Fig. 6**B** and **C**, with the optical flow magnitude expressed in millimetres per second.

The two strategies for calculating temporal profiles differ in the type of movement they emphasise: the maximum value focuses on the movement of the most active nematodes, while the mean value provides a more comprehensive overview of movement across the entire experiment. Given the detection results of the CNN model, the mean value can be relied upon, as the network does not confuse parts of the arena with the nematodes. While the network may occasionally misclassify nematodes as background, this does not affect the mean value, as their movement is excluded from its calculation, ensuring it remains a reliable indicator of overall motor activity.

To quantify the overall activity for each video and compare the stimulus-presence context with the control, three features were considered: the mean, maximum, and variance of the temporal profiles. These features were computed across the entire video dataset and are presented in Fig. 7 for the two strategies used to obtain the temporal profiles. Panels 7**A**, 7**B**, and 7**C** show the mean, maximum, and variance of the temporal profiles, emphasising the motor activity of the most active nematodes in each frame. Panels 7**D**, 7**E**, and 7**F** display the same features of the temporal profiles, highlighting the overall motor activity across the video.

Statistical analysis revealed significant features, indicating meaningful differences in motor activity and locomotion between the two groups. The mean values of the temporal profiles show significance both for profiles emphasising the motor activity of the most active nematodes ($p = 0.0162$) and those highlighting overall motor activity ($p = 0.0078$). In the latter case, the maximum ($p = 0.0055$) and variance ($p = 0.0106$) features also show significance. *Steinernema carpocapsae* exhibited a more intense activity in presence of host-borne cues.

Given that the features derived from the temporal profiles highlighting overall motor activity offered a more comprehensive view of the nematodes' behaviour across the video dataset, and due to their statistical significance, subsequent analysis focused on these. The extracted features not only captured the activity of the most active nematodes, but also the broader motor patterns throughout the experiment. Based on these features, two classifiers were trained, support vector machine and multilayer perceptron, each leveraging these key features to distinguish between the groups. This approach was utilised to differentiate the motor activity under different experimental conditions, ensuring a more robust and comprehensive analysis. Fig. 8 presents the results of the machine learning classifiers in distinguishing between stimulus and control contexts, based on the features obtained from optical flow analysis. Fig. 8**A** shows the comparison between the two classifiers using metrics such as precision, recall, accuracy, and F1-score, while Panels 8**B**

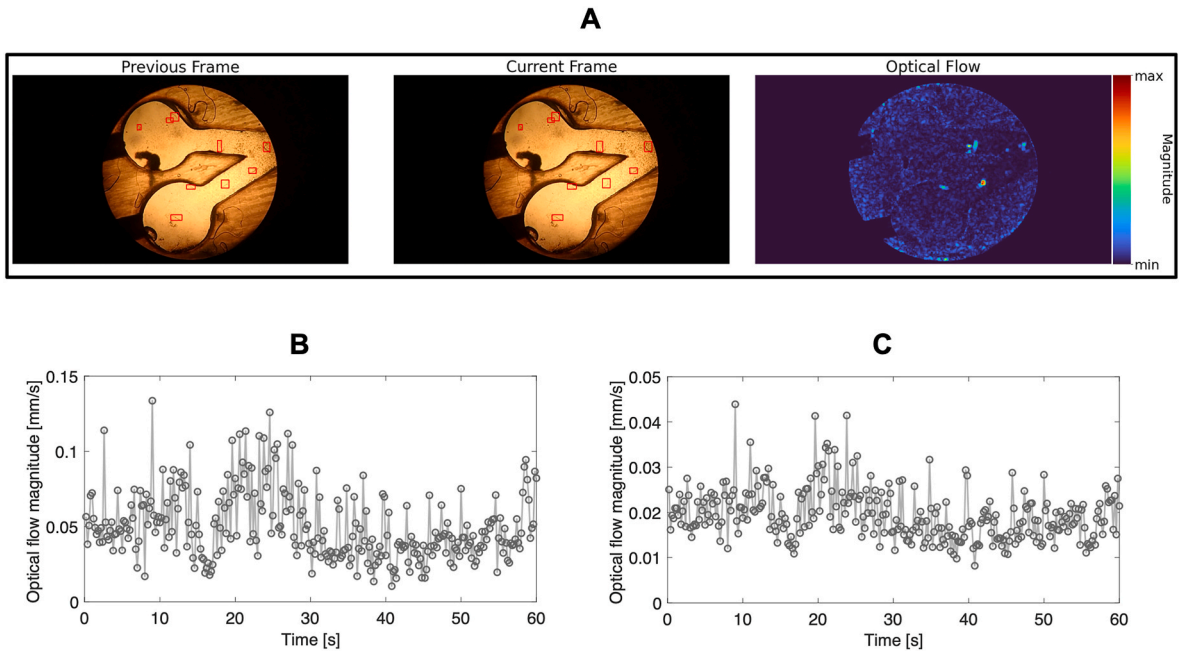

Fig. 6. Optical flow analysis: Two consecutive frames from a stimulus-context video sampled at 5 Hz, shown alongside the graphical representation of the optical flow magnitude, normalised using MIN-MAX scaling (**A**). Temporal profiles of the optical flow magnitude for the video sample, derived from the maximum (**B**) and mean (**C**) values calculated from the averaged magnitude values within the bounding boxes for each frame.

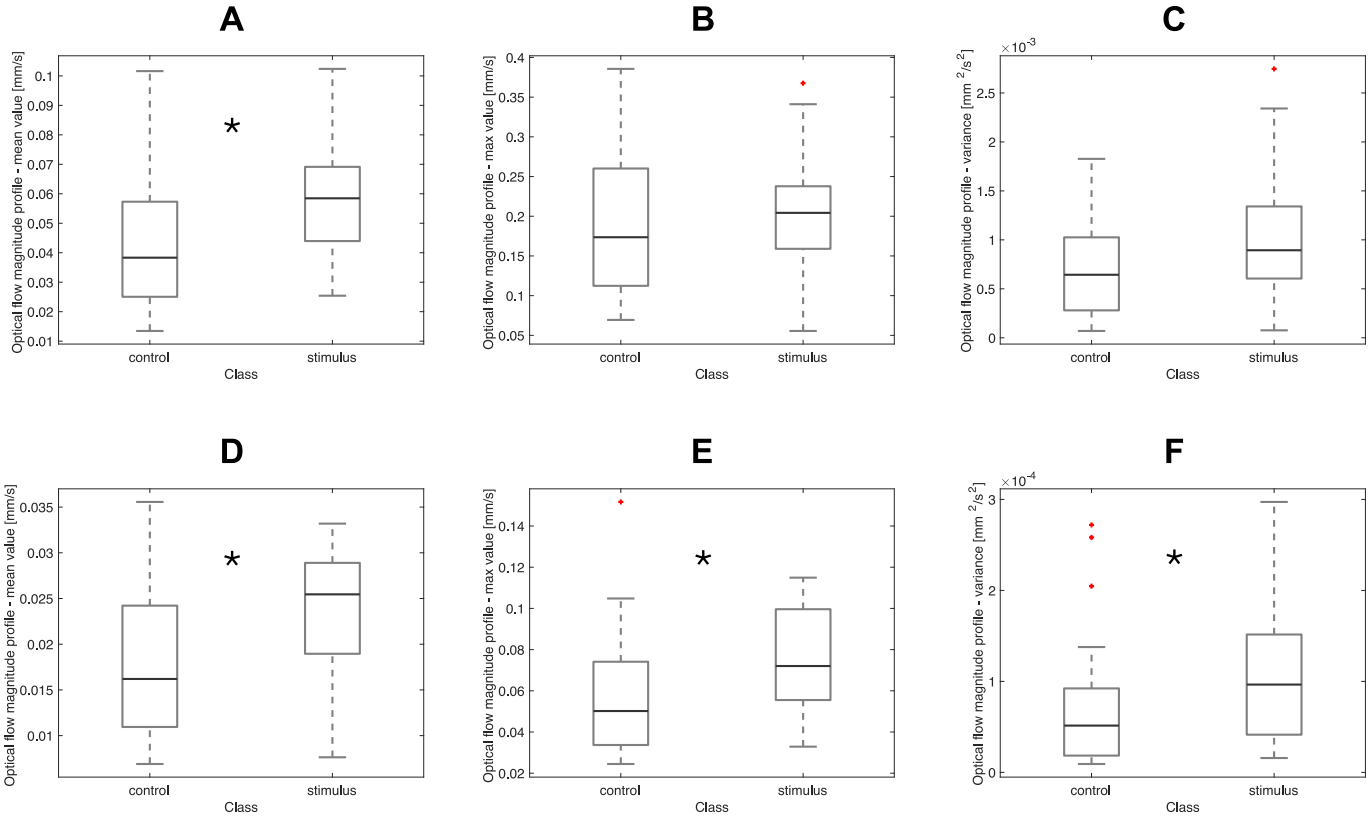

Fig. 7. Optical flow results: Features extracted from the temporal profiles across the video dataset, comparing motor activity in the stimulus-presence context with the control. Mean (**A**), maximum (**B**), and variance (**C**) of temporal profiles emphasising the motor activity of the most active nematodes in each frame, and mean (**D**), maximum (**E**), and variance (**F**) of temporal profiles highlighting overall motor activity. Asterisks (*) on the boxplots indicate statistical significance.

and 8**C** display the receiver operating characteristic curves for the SVM and MLP classifiers, respectively.

The performance results of the two classifiers indicate distinct differences in their ability to distinguish between nematodes under stimulus and control conditions. SVM classifier achieved a precision of 0.75, recall of 0.63, accuracy of 0.70, and F1-score of 0.67. MLP

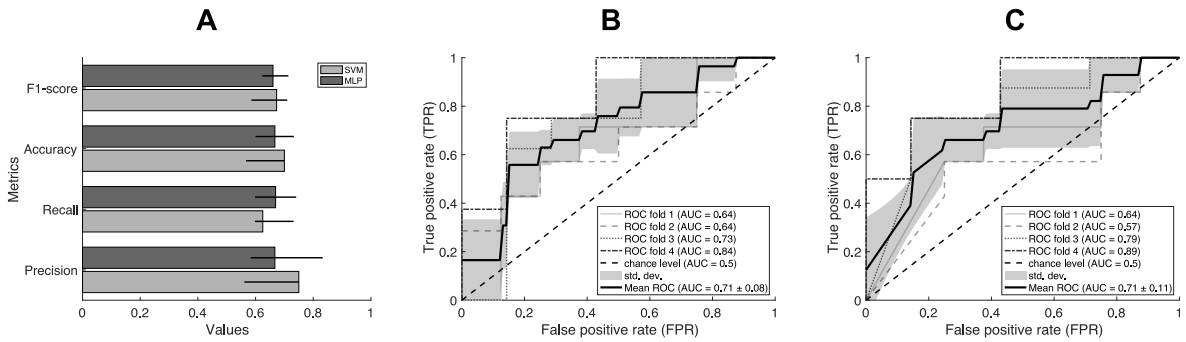

Fig. 8. Machine learning classifier performance in distinguishing between stimulus control contexts, using features derived from optical flow analysis: Comparison of the performance of two classifiers (support vector machine and multilayer perceptron) based on precision, recall, accuracy, and F1-score in terms of median and interquartile range across the 4 folds of the cross validation (**A**); receiver operating characteristic curves of SVM (**B**) and MLP (**C**) classifiers, with the corresponding area under the curve values displayed.

classifier showed slightly lower performance, with precision, recall, accuracy, and F1-score around 0.66 and 0.67. Both classifiers achieved an area under the receiver operating characteristic curve of 0.71. This score shows that both classifiers performed similarly in separating the two classes. Given these results, it is evident that both classifiers, based on the features extracted through optical flow analysis, effectively distinguish between the nematodes' motor activity in response to the presence of a stimulus compared to when no stimulus was present.

4. Discussion

Engineered testing arenas, leveraging lab-on-a-chip technology, are increasingly applied in behavioural and ecological studies (Campana & Wlodkowic, 2018; Romano et al., 2022). In the case of nematodes this technology is well established and allows to test motility and taxis in presence of different stimuli such as chemical compounds or electrical stimuli conveyed in the microchannel by means of metal electrode (Ghaemi et al., 2015). Lab-on-a-chip technology is also employed as a valid technique to drug screening by using nematode's sensing (Carr et al., 2011). Considering the growing significance within the scientific context of the lab-on-a-chip technique application (Romano et al., 2022; Shanti et al., 2018), this work provides a technological advancement in biosystems investigation and management. Lab-on-a-chip platforms are valuable for observing microscopic organisms within a device that mimics the microchannel structure of soil, while also reducing interference from environmental factors that could compromise data collection. A further advantage of microfluidics is the possibility to replicate numerous identical copies of the arena through fast prototyping techniques (Weisgrab et al., 2019), thus standardising the experimental phase to reduce the errors during the analysis of results (Haeberle & Zengerle, 2007).

The integration of AI into lab-on-a-chip solutions could be a powerful tool for a deeper analysis on behavioural patterns, gaining insights into motor activities difficult to observe with traditional approaches. The engineering approach adopted in this work based on the combination of three different tools—microfluidics, machine learning, and optical flow—is still poorly explored in the current state of the art. But the possibility to merge and integrate these tools represents a strategy capable of collecting high-quality data and enabling in-depth analysis. A preliminary study with initial results was previously presented (Manduca et al., 2024a, 2024b), but in this work, a more in-depth analysis is provided, alongside the integration of machine learning classifiers to identify changes in motor activity in response to stimuli, based on data extracted from optical flow analysis. The integration of deep learning into microfluidic platforms has been previously used for segmentation and classification tasks, such as the segmentation of channel images and the classification of adhered cells into subtypes (Praljak et al., 2021) or for tumour cell screening (Hashemzadeh et al., 2021). In this study, deep learning was employed for three distinct purposes using the same CNN model: (1) to identify target elements in an environment, (2) to differentiate and analyse their behaviour in response to stimuli, and (3) to detect the presence of stimuli in an environment based on behavioural patterns, effectively using them as biosensors. The integration of optical flow with microfluidics, on the other hand, has predominantly been applied for flow rate measurement (Garbe et al., 2006; Nguyen & Truong, 2005). In this context, optical flow enabled a detailed analysis of the motor activity of the target individuals, identified by the network. Notably, within microchannels, fluid flow is predominantly laminar due to the low Reynolds number (Schulte et al., 2002), minimising interference from medium turbulence.

Steinernema carpocapsae has been described for years as an ambusher EPN without the capability to search and move towards a potential host (Koppenhöfer & Kaya, 1996). This trait is an important issue that, despite the simple mass rearing, avoids its effective application against many constrained pests (Ehlers, 2001). More recently, it has been described as an intermediate nematode, whose motility was influenced by different habitat conditions (Kruitbos and Wilson, 2010); actually, the presence of a high percentage of organic matter in the soil (peat soil) can enhance cruising in *S. carpocapsae* (Dembilio et al., 2010). This AI and microfluidics-based investigation reveals some relevant traits of a cruiser species and enhances the knowledge of *S. carpocapsae* behaviour paving the path for its broader application as a BCA. The achieved results show differences in the motor activity in presence of a given cue and deep learning image-based method underlined variations in EPN kinesis.

The trained network showed some difficulties detecting nematodes at frame-level due to background interferences, but results may improve by using a different device set up when it is placed under the microscope. Furthermore, a more precise and efficient device for handling nematodes could enable the observation of individual specimens, improve video recording quality and the following analysis. Additionally, using a localised stimulus instead of one dispersed in a fluid medium could provide a clearer understanding of behavioural differences. Refining the microfluidic setup, such as incorporating a caging system to isolate the stimulus, along with the use of pose estimation techniques, could provide greater insight into movement patterns. Despite these limitations, the proposed approach remains a valuable tool for studying fundamental behavioural traits.

Results improved at video-level where the network achieved a precision of 1.00. The optical flow analysis integration allowed for an investigation of the motor activity over time. *Steinernema carpocapsae* showed a significant distinction among different conditions, with a more intense activity in presence of EGVM faeces. Results confirm the presence of both ambusher and cruiser behavioural traits in *S. carpocapsae* (see also Wilson et al., 2012). Indeed, differences in *S. carpocapsae* motor activity were observed depending on the presence of an attractive cue.

This confirms the possibility that *S. carpocapsae*, when perceiving chemical signals from surrounding living hosts, can actively search for it exploiting variations in klinotaxis. Taking into consideration the tested cues and earlier research on the inductive effects of the host gut on EPN's behaviour (Grewal et al., 1993), the movement of nematodes towards EGVM faeces appears to be triggered by the presence of chemical compounds with an attractive influence on their behaviour. Nematodes can perceive a chemical or physical stimulus from huge distances thanks to the sensory organs displaced at both ends of the body, their main responses consist of taxis and changes in body conformation (Robinson & Perry, 2006). Their cue sensing and their motility attitude had been assessed by using several approaches, some of them are able to reproduce EPN's natural habitat (Shapiro-Ilan et al., 2014), where specimens were tested by using sandy soil that according to Powers et al. (2009) is not the ideal habitat for *S. carpocapsae*.

The chemotactic response of soil nematodes has been studied by observing its crawling movements across a chemical gradient on agar Petri dishes (Ward, 1973); unfortunately, this approach led to an unstable gradient of compounds. An earlier study also relied on microchannel devices, where chemical gradients of an attractive, or repellent compound, are maintained, thanks to the diffusion in a fluid relying on the laminar flow typical of microfluidics systems (Chronis et al., 2007). Leveraging on previous knowledge, the proposed approach mimics EPN living conditions, within a microfluidic platform that adds the capability to work with a compact and reproducible device that limits the possibility of significant error. Considering the importance of movement and locomotion in EPN's survival, behavioural assessments are commonly based on EPN-host interaction. In this study, faeces of EGVM larvae were used, and data were analysed through the application of AI and computer vision without needing an operator.

Within the *Steinernema* genus there are both cruiser and ambusher species. Ambusher nematodes are characterised by a peculiar movement known as "nictation" where specimens stand up on their tail to reach a potential host who is passing by (Campbell & Gaugler, 1993). However, a possible cruiser attitude had been considered by Lewis et al. (1992). Considering only the ambusher behaviour of this species can be counterproductive, as it limits its application to insect pests with a high level of motility (Lalitha et al., 2022; Yan et al., 2020). Given the growing interest in developing more effective strategies against invasive pests, our findings highlight a degree of motility and taxis in *S. carpocapsae*, supporting its potential application in managing a wider range of pest species. Its ability to actively locate hosts or host-derived cues is crucial for enhancing its entomopathogenic activity. In support of the evidence that *S. carpocapsae* may behave as a "cruiser", earlier studies provide valuable insights. For instance, Lacey et al. (2006) conducted experiments using EPNs to control cocooned larvae of *Cydia pomonella* (L.) (Lepidoptera: Tortricidae) on pear and apple logs, as well as within leaf litter. Their findings revealed that the "ambusher" *S. carpocapsae* outperformed the "cruiser" *Heterorhabditis bacteriophora* Poinar (Rhabditida: Heterorhabditidae) in eliminating these immobile insect stages in both scenarios. Martinez de Altube et al. (2008) conducted field trials employing *S. carpocapsae* in a chitosan formulation, achieving significant control rates against the flat-headed root borer *Capnodis tenebrionis* (L.) (Coleoptera: Buprestidae). *Steinernema carpocapsae* were used also in a chitosan formulation, achieving high values of control of the Red Palm Weevil, *Rhynchophorus ferrugineus* (Olivier) (Coleoptera: Dryophthoridae), larvae (Dembilio et al., 2010). The authors found that *S. carpocapsae* actively penetrates the palm crown rather than remaining outside and waiting for the host. In this study, a fully automated approach was proposed to deeper investigate motor differences in presence of a suitable host. All the knowledge arising from the present study can be useful in other fields of research, such as medical diagnostics, where nematodes have been shown to detect chemical compounds directly linked to cancer development (Zhang et al., 2023). Moreover, coupling a similar approach of detection to genetic technologies would make possible the developments of modified strains able to be employed as biosensors for heavy metal early detection with a huge positive impact on safety and environmental conservation (Anbalagan et al., 2012).

5. Conclusions

The experimental apparatus and the multidisciplinary approach developed has facilitated the microscopic observation of EPNs through assessments under the inverted microscope. Deep learning and computer vision analyses were essential to stress differences in movement patterns (posture) and locomotion towards a host-borne cue, which assume kairomonal significance. The CNN model succeeded in the discrimination of the two groups of nematodes (control and stimulus-exposed EPNs) from an image comparison while the optical flow integration deeper investigated the motor activity evaluating the movement over time. This investigation provides a comprehensive understanding of the behaviour of *S. carpocapsae*, supporting its classification as a cruiser species. This inference holds significant relevance, given the employed methodology and its potential implications for biocontrol. The developed approach could be utilised to study the response of EPNs to various agricultural pests, for potentially enhancing the efficacy of this BCA in sustainable pest management. Furthermore, by correlating a specific movement pattern of the nematode with the presence of a particular phytophagous pest or chemical cue(s), it could function as a biosensor, facilitating an early detection of the pest with a consequent positive impact on integrated pest management practices.

Funding

This study was carried out in the framework of the EU H2020 FETOPEN Project "Robocoenosis - ROBOts in cooperation with a bioCOENOSIS'' [899520], the Italian Ministry of Education, University and Research, PRIN Project "COSMIC—COntrolled Space MIcro-ecological system supporting eCopoiesis" [2022EY5BXC], the EU HORIZON PATHFINDEROPEN Project 'SENSORBEES– Sensorbees are ENhanced Self-ORganizing Biohybrids for Ecological and Environmental Surveillance' [101130325], and the Italian National Biodiversity Future Center [CN00000033]. Funders had no role in the study design, data collection and analysis, decision to publish, or preparation of the manuscript.

CRediT authorship contribution statement

Gianluca Manduca: Writing – review & editing, Writing – original draft, Visualization, Software, Methodology, Investigation, Formal analysis, Data curation, Conceptualization. **Valeria Zeni:** Writing – review & editing, Investigation, Formal analysis, Data curation. **Anita Casadei:** Writing – review & editing, Writing – original draft, Investigation, Formal analysis, Data curation. **Eustachio Tarasco:** Writing – review & editing, Resources, Formal analysis. **Andrea Lucchi:** Writing – review & editing, Resources, Formal analysis. **Giovanni Benelli:** Writing – review & editing, Resources, Methodology, Formal analysis. **Cesare Stefanini:** Writing – review & editing, Resources, Formal analysis. **Donato Romano:** Writing – review & editing, Writing – original draft, Validation, Supervision, Resources, Project administration, Methodology, Investigation, Funding acquisition, Formal analysis, Conceptualization.

Declaration of competing interest

The authors declare that they have no known competing financial interests or personal relationships that could have appeared to influence the work reported in this paper.

Acknowledgment

The authors thank Federica Durini and Cristina Piras for their kind assistance in visualization.

References

Alhothali, A., Balabid, A., Alharthi, R., Alzahrani, B., Alotaibi, R., & Barnawi, A. (2023). Anomalous event detection and localization in dense crowd scenes. *Multimedia Tools and Applications, 82*(10), 15673–15694. https://doi.org/10.1007/s11042-022-13967-w

Anbalagan, C., Lafayette, I., Antoniou-Kourounioti, M., Haque, M., King, J., Johnsen, B., & De Pomerai, D. (2012). Transgenic nematodes as biosensors for metal stress in soil pore water samples. *Ecotoxicology, 21*, 439–455. https://doi.org/10.1007/s10646-011-0804-0

Baiocchi, T., Lee, G., Choe, D. H., & Dillman, A. R. (2017). Host seeking parasitic nematodes use specific odors to assess host resources. *Scientific Reports, 7*(1), 6270. https://doi.org/10.1038/s41598-017-06620-2

Benelli, G., Lucchi, A., Anfora, G., Bagnoli, B., Botton, M., Campos-Herrera, R., Carlos, C., Daugherty, M. P., Gemeno, C., Harari, A. R., Hoffmann, C., Ioriatti, C., López Plantey, R. J., Reineke, A., Ricciardi, R., Roditakis, E., Simmons, G. S., Tay, W. T., Torres-Vila, L. M., Vontas, J., & Thiery, D. (2023a). European grapevine moth, *Lobesia botrana* Part I: Biology and ecology. *Entomologia Generalis, 43*(2), 261–280. https://doi.org/10.1127/entomologia/2023/1837

Benelli, G., Lucchi, A., Anfora, G., Bagnoli, B., Botton, M., Campos-Herrera, R., Carlos, C., Daugherty, M. P., Gemeno, C., Harari, A. R., Hoffmann, C., Ioriatti, C., López Plantey, R. J., Reineke, A., Ricciardi, R., Roditakis, E., Simmons, G. S., Tay, W. T., Torres-Vila, L. M., Vontas, J., & Thiery, D. (2023b). European grapevine moth, *Lobesia botrana* Part II: Prevention and management methods. *Entomologia Generalis, 43*(2), 281–304. https://doi.org/10.1127/entomologia/2023/1947

Benelli, G., Pavoni, L., Zeni, V., Ricciardi, R., Cosci, F., Cacopardo, G., Gendusa, S., Spinozzi, E., Petrelli, R., Cappellacci, L., Maggi, F., Pavela, R., Bonacucina, G., & Lucchi, A. (2020). Developing a highly stable *Carlina acaulis* essential oil nanoemulsion for managing *Lobesia botrana*. *Nanomaterials, 10*, 1867. https://doi.org/10.3390/nano10091867

Buckingham, S. D., Partridge, F. A., & Sattelle, D. B. (2014). Automated, high throughput, motility analysis in *Caenorhabditis elegans* and parasitic nematodes: Applications in the search for new anthelmintics. *International Journal for Parasitology: Drugs and Drug Resistance, 4*(3), 226–232. https://doi.org/10.1016/j.ijpddr.2014.10.004

Campana, O., & Wlodkowic, D. (2018). The undiscovered country: Ecotoxicology meets microfluidics. *Sensors and Actuators B: Chemical, 257*, 692–704. https://doi.org/10.1016/j.snb.2017.11.002

Campbell, J. F., & Gaugler, R. (1993). Nictation behaviour and its ecological implications in the host search strategies of entomopathogenic nematodes (Heterorhabditidae and Steinernematidae). *Behaviour, 126*(3–4), 155–169. https://doi.org/10.1163/156853993X00092

Campbell, J. F., & Gaugler, R. R. (1997). Inter-specific variation in entomopathogenic nematode foraging strategy: Dichotomy or variation along a continuum. *Fundamental and Applied Nematology, 20*(4), 393–398. https://www.scopus.com/inward/record.uri?eid=2-s2.0-0030804728&partnerID=40&md5=12c0edc10f1c37589d3f54773a1b44f4.

Carr, J. A., Parashar, A., Gibson, R., Robertson, A. P., Martin, R. J., & Pandey, S. (2011). A microfluidic platform for high-sensitivity, real-time drug screening on *C. elegans* and parasitic nematodes. *Lab on a Chip, 11*(14), 2385–2396. https://doi.org/10.1039/C1LC20170K

Chronis, N., Zimmer, M., & Bargmann, C. I. (2007). Microfluidics for in vivo imaging of neuronal and behavioral activity in *Caenorhabditis elegans*. *Nature Methods, 4*(9), 727–731. https://doi.org/10.1038/nmeth1075

Conde, J. P., Madaboosi, N., Soares, R. R., Fernandes, J. T. S., Novo, P., Moulas, G., & Chu, V. (2016). Lab-on-chip systems for integrated bioanalyses. *Essays in Biochemistry, 60*(1), 121–131. https://doi.org/10.1042/EBC20150013

Dembilio, O., Llacer, E., Martínez de Altube, M. D. M., & Jacas, J. A. (2010). Field efficacy of imidacloprid and *Steinernema carpocapsae* in a chitosan formulation against the red palm weevil *Rhynchophorus ferrugineus* (Coleoptera: Curculionidae) in *Phoenix canariensis*. *Pest Management Science: Formerly Pesticide Science, 66*(4), 365–370. https://doi.org/10.1002/ps.1882

Ehlers, R. U. (2001). Mass production of entomopathogenic nematodes for plant protection. *Applied Microbiology and Biotechnology, 56*, 623–633. https://doi.org/10.1007/s002530100711

Farnebäck, G. (2003). Two-frame motion estimation based on polynomial expansion. In *Image analysis: 13th Scandinavian Conference, SCIA 2003 Halmstad, Sweden, June 29–July 2, 2003 proceedings* (Vol. 13, pp. 363–370). Springer Berlin Heidelberg. https://doi.org/10.1007/3-540-45103-X_50.

Fatichah, C., Alam, S. P., & Navastara, D. A. (2019). Optical flow feature based for fire detection on video data. In *2019 1st International Conference on artificial intelligence and data sciences (AiDAS)* (pp. 100–105). https://doi.org/10.1109/AiDAS47888.2019.8970957. Ipoh, Malaysia.

Fazzari, E., Romano, D., Falchi, F., & Stefanini, C. (2025). Selective state models are what you need for animal action recognition. *Ecological Informatics, 85*, 102955. https://doi.org/10.1016/j.ecoinf.2024.102955

Ferreira, F. R. T., do Couto, L. M., & de Melo Baptista Domingues, G. (2024). Exploring the potential of YOLOv8 in hybrid models for facial mask identification in diverse environments. *Neural Computing & Applications, 36*, 22037–22052. https://doi.org/10.1007/s00521-024-10351-7

Ferreira, J. J., Lopes, J. M., Gomes, S., & Rammal, H. G. (2023). Industry 4.0 implementation: Environmental and social sustainability in manufacturing multinational enterprises. *Journal of Cleaner Production, 404*, Article 136841. https://doi.org/10.1016/j.jclepro.2023.136841

Gang, S. S., & Hallem, E. A. (2016). Mechanisms of host seeking by parasitic nematodes. *Molecular and Biochemical Parasitology, 208*(1), 23–32. https://doi.org/10.1016/j.molbiopara.2016.05.007

Garbe, C., Roetmann, K., & Jähne, B. (2006). An optical flow based technique for the non-invasive measurement of microfluidic flows. In *12th International Symposium on flow visualization*. https://doi.org/10.11588/heidok.00018182

Garmasukis, R., Hackl, C., Charvat, A., Mayr, S. G., & Abel, B. (2023). Rapid prototyping of microfluidic chips enabling controlled biotechnology applications in microspace. *Current Opinion in Biotechnology, 81*, Article 102948. https://doi.org/10.1016/j.copbio.2023.102948

Gaugler, R. (1988). Ecological considerations in the biological control of soil-inhabiting insects with entomopathogenic nematodes. *Agriculture, Ecosystems & Environment, 24*(1–3), 351–360. https://doi.org/10.1016/0167-8809(88)90078-3

Ghaemi, R., Rezai, P., Iyengar, B. G., & Selvaganapathy, P. R. (2015). Microfluidic devices for imaging neurological response of *Drosophila melanogaster* larva to auditory stimulus. *Lab on a Chip, 15*(4), 1116–1122. https://doi.org/10.1039/C4LC01245C

Grewal, P. S., Gaugler, R., & Selvan, S. (1993). Host recognition by entomopathogenic nematodes: Behavioral response to contact with host feces. *Journal of Chemical Ecology, 19*, 1219–1231. https://doi.org/10.1007/BF00987382

Haeberle, S., & Zengerle, R. (2007). Microfluidic platforms for lab-on-a-chip applications. *Lab on a Chip, 7*(9), 1094–1110. https://doi.org/10.1039/B706364B

Hashemzadeh, H., Shojaeilangari, S., Allahverdi, A., Rothbauer, M., Ertl, P., & Naderi-Manesh, H. (2021). A combined microfluidic deep learning approach for lung cancer cell high throughput screening toward automatic cancer screening applications. *Scientific Reports, 11*(1), 9804. https://doi.org/10.1038/s41598-021-89352-8

Huangfu, Z., & Li, S. (2023). Lightweight you only look once v8: An upgraded you only look once v8 algorithm for small object identification in unmanned aerial vehicle images. *Applied Sciences, 13*, Article 12369. https://doi.org/10.3390/app132212369

Jagodič, A., Ipavec, N., Trdan, S., & Laznik, Ž. (2017). Attraction behaviors: Are synthetic volatiles, typically emitted by insect-damaged *Brassica nigra* roots, navigation signals for entomopathogenic nematodes (*Steinernema* and *Heterorhabditis*). *BioControl, 62*, 515–524. https://doi.org/10.1007/s10526-017-9796-x

Johnston, I. D., McCluskey, D. K., Tan, C. K., & Tracey, M. C. (2014). Mechanical characterization of bulk Sylgard 184 for microfluidics and microengineering. *Journal of Micromechanics and Microengineering, 24*(3), Article 035017. https://doi.org/10.1088/0960-1317/24/3/035017

Koppenhöfer, A. M., & Kaya, H. K. (1996). Coexistence of two steinernematid nematode species (Rhabditida: Steinernematidae) in the presence of two host species. *Applied Soil Ecology, 4*(3), 221–230. https://doi.org/10.1016/S0929-1393(96)00121-7

Kruitbos, L. M., & Wilson, M. J. (2010). Is it time to wave goodbye to nictating nematodes. *Nematology, 12*, 309–310. https://doi.org/10.1163/138855409X12506855979794

Lacey, L. A., Arthurs, S. P., Unruh, T. R., Headrick, H., & Fritts Jr, R. (2006). Entomopathogenic nematodes for control of codling moth (Lepidoptera: Tortricidae) in apple and pear orchards: Effect of nematode species and seasonal temperatures, adjuvants, application equipment, and post-application irrigation. *Biological Control, 37*(2), 214–223. https://doi.org/10.1016/j.biocontrol.2005.09.015

Lalitha, K., Venkatesan, S., Balamuralikrishnan, B., & Shivakumar, M. S. (2022). Isolation and biocontrol efficacy of entomopathogenic nematodes *Steinernema carpocapsae, Steinernema monticolum* and *Rhabditis blumi* on lepidopteran pest *Spodoptera litura*. *Biocatalysis and Agricultural Biotechnology, 39*, Article 102291. https://doi.org/10.1016/j.bcab.2022.102291

Lewis, E. E., Gaugler, R., & Harrison, R. (1992). Entomopathogenic nematode host finding: Response to host contact cues by cruise and ambush foragers. *Parasitology, 105*(2), 309–315. https://doi.org/10.1017/S0031182000074230

Manduca, G., Casadei, A., Zeni, V., Benelli, G., Stefanini, C., & Romano, D. (2024a). Insights into entomopathogenic nematode behavior by using AI techniques to advance sustainable pest control. In *Ceur workshop proceedings* (Vol. 3762)CEUR-WS. https://ceur-ws.org/Vol-3762/483.pdf.

Manduca, G., Padovani, L., Carosio, E., Graziani, G., Stefanini, C., & Romano, D. (2023a). Development of an autonomous fish-inspired Robotic platform for Aquaculture inspection and management. In *2023 IEEE International Workshop on Metrology for agriculture and Forestry (MetroAgriFor)* (pp. 188–193). https://doi.org/10.1109/MetroAgriFor58484.2023.10424093. Pisa, Italy, 2023.

Manduca, G., Zeni, V., Casadei, A., Benelli, G., Stefanini, C., & Romano, D. (2024b). Integrating microfluidics and deep learning to investigate entomopathogenic nematode responses to host cues. In *2024 46th Annual International Conference of the IEEE engineering in medicine and biology society (EMBC)* (pp. 1–4). https://doi.org/10.1109/EMBC53108.2024.10782918. Orlando, FL, USA, 2024.

Manduca, G., Zeni, V., Moccia, S., Milano, B. A., Canale, A., Benelli, G., Stefanini, C., & Romano, D. (2023b). Learning algorithms estimate pose and detect motor anomalies in flies exposed to minimal doses of a toxicant. *iScience, 26*(12). https://doi.org/10.1016/j.isci.2023.108349

Martinez de Altube, M. D. M., Strauch, O., Fernandez De Castro, G., & Martinez Peña, A. (2008). Control of the flat-headed root borer *Capnodis tenebrionis* (Linné) (Coleoptera: Buprestidae) with the entomopathogenic nematode *Steinernema carpocapsae* (Weiser)(Nematoda: Steinernematidae) in a chitosan formulation in apricot orchards. *BioControl, 53*(3), 531–539. https://doi.org/10.1007/s10526-007-9094-0

Mesías-Ruiz, G. A., Pérez-Ortiz, M., Dorado, J., De Castro, A. I., & Peña, J. M. (2023). Boosting precision crop protection towards agriculture 5.0 via machine learning and emerging technologies: A contextual review. *Frontiers in Plant Science, 14*, Article 1143326. https://doi.org/10.3389/fpls.2023.1143326

Mumtaz, N., Ejaz, N., Habib, S., Mohsin, S. M., Tiwari, P., Band, S. S., & Kumar, N. (2023). An overview of violence detection techniques: Current challenges and future directions. *Artificial Intelligence Review, 56*, 4641–4666. https://doi.org/10.1007/s10462-022-10285-3

Nguyen, N. T., & Truong, T. Q. (2005). Flow rate measurement in microfluidics using optical sensors. In *Proc. 1st Int. Conf. Sensing Technol.*.

Ping, P., Huang, C., Ding, W., Liu, Y., Chiyomi, M., & Kazuya, T. (2023). Distracted driving detection based on the fusion of deep learning and causal reasoning. *Information Fusion, 89*, 121–142. https://doi.org/10.1016/j.inffus.2022.08.009

Powers, T. O., Neher, D. A., Mullin, P., Esquivel, A., Giblin-Davis, R. M., Kanzaki, N., Stock, S. P., Mora, M. M., & Uribe-Lorio, L. (2009). Tropical nematode diversity: Vertical stratification of nematode communities in a Costa Rican humid lowland rainforest. *Molecular Ecology, 18*(5), 985–996. https://doi.org/10.1111/j.1365-294X.2008.04075.x

Praljak, N., Iram, S., Goreke, U., Singh, G., Hill, A., Gurkan, U. A., & Hinczewski, M. (2021). Integrating deep learning with microfluidics for biophysical classification of sickle red blood cells adhered to laminin. *PLoS Computational Biology, 17*(11), Article e1008946. https://doi.org/10.1371/journal.pcbi.1008946

Robinson, A. F., & Perry, R. N. (2006). Behavior and sensory perception. https://doi.org/10.1079/9781845930561.0210.

Romano, D., Rossetti, G., & Stefanini, C. (2022). Learning on a chip: Towards the development of trainable biohybrid sensors by investigating cognitive processes in non-marine Ostracoda via a miniaturised analytical system. *Biosystems Engineering, 213*, 162–174. https://doi.org/10.1016/j.biosystemseng.2021.11.004

Santaera, G., Zeni, V., Manduca, G., Canale, A., Mele, M., Benelli, G., Stefanini, C., & Romano, D. (2025). Development of an autonomous smart trap for precision monitoring of hematophagous flies on cattle. *Smart Agricultural Technology, 10*, Article 100842. https://doi.org/10.1016/j.atech.2025.100842

Schulte, T. H., Bardell, R. L., & Weigl, B. H. (2002). Microfluidic technologies in clinical diagnostics. *Clinica Chimica Acta, 321*(1–2), 1–10. https://doi.org/10.1016/S0009-8981(02)00093-1

Sengupta, J., & Hussain, C. M. (2022). Prospective pathways of green graphene-based lab-on-chip devices: The pursuit toward sustainability. *Microchimica Acta, 189*(5), 177. https://doi.org/10.1007/s00604-022-05286-6

Shanti, A., Teo, J., & Stefanini, C. (2018). In vitro immune organs-on-chip for drug development: A review. *Pharmaceutics, 10*(4), 278. https://doi.org/10.3390/pharmaceutics10040278

Shapiro-Ilan, D. I., Lewis, E. E., & Schliekelman, P. (2014). Aggregative group behavior in insect parasitic nematode dispersal. *International Journal for Parasitology, 44*(1), 49–54. https://doi.org/10.1016/j.ijpara.2013.10.002

Shinde, S. V., Patel, J. I., & Purohit, M. S. (2010). Report of entomopathogenic nematode, *Steinernema carpocapsae* (Weiser)(Nematoda: Steinernematidae) from North Gujarat. *Journal of Biological Control*, 75–76.

Stuart, R. J., Barbercheck, M. E., & Grewal, P. S. (2015). Entomopathogenic nematodes in the soil environment: Distributions, interactions and the influence of biotic and abiotic factors. *Nematode Pathogenesis of Insects and Other Pests: Ecology and Applied Technologies for Sustainable Plant and Crop Protection*, 97–137. https://doi.org/10.1007/978-3-319-18266-7_4

Tarasco, E., Fanelli, E., Salvemini, C., El-Khoury, Y., Troccoli, A., Vovlas, A., & De Luca, F. (2023). Entomopathogenic nematodes and their symbiotic bacteria: From genes to field uses. *Frontiers in Insect Science, 3*, Article 1195254. https://doi.org/10.3389/finsc.2023.1195254

Terven, J., Córdova-Esparza, D. M., & Romero-González, J. A. (2023). A comprehensive review of yolo architectures in computer vision: From yolov1 to yolov8 and yolo-nas. *Machine Learning and Knowledge Extraction, 5*(4), 1680–1716. https://doi.org/10.3390/make5040083

Ward, S. (1973). Chemotaxis by the nematode *Caenorhabditis elegans*: Identification of attractants and analysis of the response by use of mutants. *Proceedings of the National Academy of Sciences, 70*(3), 817–821. https://doi.org/10.1073/pnas.70.3.817

Weisgrab, G., Ovsianikov, A., & Costa, P. F. (2019). Functional 3D printing for microfluidic chips. *Advanced Materials Technologies, 4*(10), Article 1900275. https://doi.org/10.1002/admt.201900275

Wilson, M. J., Ehlers, R. U., & Glazer, I. (2012). Entomopathogenic nematode foraging strategies–is *Steinernema carpocapsae* really an ambush forager? *Nematology, 14*(4), 389–394. https://doi.org/10.1163/156854111X617428

Wolozin, B., Gabel, C., Ferree, A., Guillily, M., & Ebata, A. (2011). Watching worms whither: Modeling neurodegeneration in C. elegans. *Progress in Molecular Biology and Translational Science, 100*, 499–514. https://doi.org/10.1016/B978-0-12-384878-9.00015-7

Yan, J. J., Sarkar, S. C., Meng, R. X., Reitz, S., & Gao, Y. L. (2020). Potential of *Steinernema carpocapsae* (Weiser) as a biological control agent against potato tuber moth, *Phthorimaea operculella* (Zeller)(Lepidoptera: Gelechiidae). *Journal of Integrative Agriculture, 19*(2), 389–393. https://doi.org/10.1016/S2095-3119(19)62826-1

Zhang, J., Li, W., Huang, Q., Fu, Y., Liu, Y., Luo, X., Zou, S., Chua, S. L., Leung, S., & Khoo, B. L. (2023). Label-free biosensor for non-invasive and low-cost detection of metastatic risk through urine biopsy. *Sensors and Actuators B: Chemical, 395*, Article 134485. https://doi.org/10.1016/j.snb.2023.134485

Zhang, X., Li, L., Kesner, L., & Robert, C. A. M. (2021). Chemical host-seeking cues of entomopathogenic nematodes. *Current Opinion in Insect Science, 44*, 72–81. https://doi.org/10.1016/j.cois.2021.03.011